Lasers in Manufacturing Conference 2019

Laser beam welding of Ti-6Al-4V hybrid-parts from additively manufactured elements and sheet metal

Florian Huber[a,c,d*], Vincent Mann[b], Florian Kaufmann[b], Michael Schmidt[a,b,c,d]

[a]*Institute of Photonic Technologies, Friedrich-Alexander-Universität Erlangen-Nürnberg, Konrad-Zuse-Straße 3/5, 91052 Erlangen, Germany*
[b]*Bayerisches Laserzentrum GmbH, Konrad-Zuse-Straße 2/6, 91052 Erlangen, Germany*
[c]*Erlangen Graduate School in Advanced Optical Technologies (SAOT), Paul-Gordan-Straße 6, 91052 Erlangen, Germany*
[d]*Collaborative Research Center 814 – Additive Manufacturing, Am Weichselgarten 9, 91058 Erlangen, Germany*

Abstract

Aim of this work is to investigate joining of additively manufactured Ti-6Al-4V with conventionally manufactured Ti-6Al-4V by laser beam welding. In this context the influence of different heat-treatment conditions on the joint strength is examined. The samples were analyzed by optical microscopy on polished and etched cross-sections and by microhardness measurements. Furthermore tensile test were performed to evaluate the mechanical strength of the samples. In dependence of the heat-treatment condition an average ultimate tensile strength of up to 866 MPa was measured for joints between L-PBF material and conventional hot rolled sheet metal. Hence, the joint strength is in good accordance with reference samples consisting of laser welded sheet metal parts reaching only a slightly higher average ultimate tensile strength of 912 MPa. However, the standard deviation (n=10) of the joint strength is increased from 8 MPa for the reference group to 41 MPa for the L-PBF/sheet metal joints.

Keywords: Additive Manufacturing, Laser Beam Welding, Ti-6Al-4V, Laser Powder Bed Fusion (L-PBF)

* Corresponding author. Tel.: +49-913-185-232-41;
E-mail address: florian.huber@lpt.uni-erlangen.de .

1. Introduction and state of the art

Additive manufacturing (AM) is currently gaining an increasing importance in industry (Wohlers, Caffrey, and Campbell 2016). By producing parts layer by layer on basis of digital data complex geometries can be fabricated without the need of product specific tools. This offers a flexible manufacturing approach for e.g. individualized parts or high-performance parts for various applications ranging from industry (Uhlmann et al. 2015) to medical (Jardini et al. 2014). The most widely used process for AM of metals is laser powder bed fusion (L-PBF) (Wohlers, Caffrey, and Campbell 2016). The basic process schema is shown in Fig. 1. L-PBF facilitates processing of a wide range of alloys like stainless steels (Lavery et al. 2017), aluminum alloys (Brandl et al. 2012) or nickel-base alloys (Sadowski et al. 2016). Due to their superior strength to weight ratio, corrosion resistance and biocompatibility (Leyens and Peters 2003) titanium alloys are especially interesting for AM applications. These excellent material properties of titanium alloys in combination with the freedom in design offered by L-PBF allows the production of highly optimized parts.

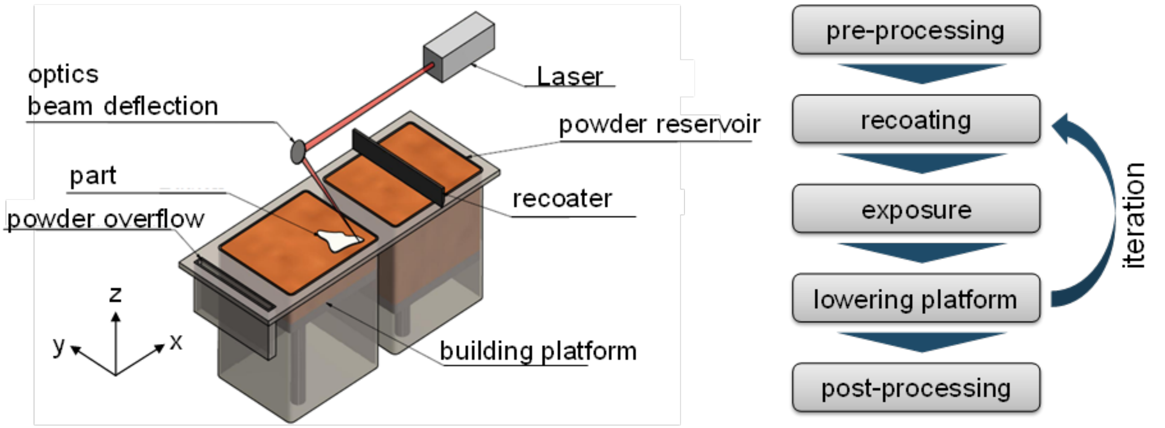

Fig. 1. Basic process schema for L-PBF of metals

However, despite its advantages L-PBF faces, several restrictions. Firstly, the maximum part dimensions are limited by the available build envelope of the machine. Current L-PBF machines feature build envelope dimensions ranging from about 100 mm (EOS GmbH 2019) to 500 mm (SLM Solutions GmbH 2019). The largest commercial L-PBF machine is offered by Concept Laser GmbH (Lichtenfels, Germany) with a build envelope of 800 x 400 x 500 mm³ (Concept Laser GmbH 2019), thus defining the maximum manufacturable parts size of L-PBF parts. In addition to the restricted maximum part size, the L-PBF process is relatively slow and expansive compared to most conventional manufacturing technologies like sheet metal forming, casting or milling (Baumers et al. 2016). Hence, for manufacturing larger parts novel solutions need to be developed. To overcome the drawbacks of a limited part size and slow build rates, manufacturing of hybrid-parts from L-PBF and conventionally manufactured elements can be an attractive solution to exploit the benefits of two manufacturing technologies. This would allow to manufacture the bulk of a part conventionally and apply additive manufacturing only where necessary. These hybrid-manufacturing approaches are already investigated e.g. for the combination of L-PBF and milling, for L-PBF and forging (Rosswag GmbH 2017) or for L-PBF and sheet metal forming (Huber et al. 2019). All these approaches have in common, that a conventionally manufactured base body was prepared, positioned in the build envelope of an L-PBF machine and an L-PBF structure was built on top of the base body. This is promising for speeding up the overall process route and allows the functionalization and customization of conventionally manufactured components by AM. Nevertheless, the build envelope restriction remains, since the whole base body has to be positioned in the L-PBF machine. Furthermore, a flat surface is required to build upon and hence L-PBF on complexly shaped three-dimensional surfaces is limited.

In this context, the availability of a capable joining technology for metal AM-parts and conventionally manufactured parts would provide another alternative for producing hybrid-parts and for realizing part sizes exceeding the build envelop of typical L-PBF machines. For this purpose, laser beam welding of Ti-6Al-4V is investigated. The alloy Ti-6Al-4V is the most common titanium alloy and is widely used for L-PBF (Herzog et al. 2016). Welding of Ti-6Al-4V is in general feasible and well investigated for conventionally manufactured material (Akman et al. 2009). However, during L-PBF the material faces cooling rates in the range of 10^5 – 10^6 K/s, which are significantly higher than at conventional manufacturing processes. This results in non-equilibrium α’-martensitic microstructures (Thijs et al. 2010) that have different physical properties than conventionally manufactured Ti-6Al-4V and might have an influence on the welding process. Furthermore, with respect to practical application a heat-treatment has to be considered in conjunction with L-PBF. This is common to remove the process inherent internal stress and to adjust the microstructure and mechanical properties (Vilaro, Colin, and Bartout 2011). It is expected, that the order in which the process steps heat-treatment and welding are undertaken has an influence on the resulting properties of the weld seam and is hence investigated.

2. Aims and Methods

Aim of this work is to investigate the influence of different sequences of heat-treatments and laser beam welding on the resulting quality of joints between additively manufactured Ti-6Al-4V and conventionally manufactured Ti-6Al-4V sheet metal. For this purpose, seven groups of samples each consisting of ten tensile test samples and one sample for metallographic investigations were prepared. For four groups AM material was welded with hot-rolled sheet metal with heat-treatments before welding, after welding and before and after welding. One group was welded without any heat-treatment. To identify the effects of L-PBF on the joint quality also three groups consisting only of hot-rolled sheet metal were welded. The heat-treatments were performed before and after welding and for one group no heat-treatment was performed at all. Furthermore one group of sheet metal was tested without welding and heat-treating as a reference group.

Table 1. Sample groups investigated within this work

Description	Abbreviation	Number of samples
Sheet metal + AM material, no heat-treatment	SM + AM, no HT	10 + 1
Sheet metal + AM material, heat-treatment after welding	SM + AM, HT after	10 + 1
Sheet metal + AM material, heat-treatment prior to and after welding	SM + AM, HT prior and after	10 + 1
Sheet metal + AM material, heat-treatment prior to welding	SM + AM, HT prior	10 + 1
Sheet metal + sheet metal, no heat-treatment	SM, no HT	10 + 1
Sheet metal + sheet metal, heat-treatment after welding	SM, HT after	10 + 1
Reference, no welding, no heat-treatment	Ref, no HT	10

The sheet metal samples were prepared by laser beam cutting from a hot rolled plate with a thickness of 2 mm. The L-PBF samples were built using an SLM 280^{HL} L-PBF machine from SLM Solutions GmbH (Lübeck, Germany). The parameter set that was applied for producing the parts was taken from previous work (Huber et al. 2019) and is shown in Table 2. The parameter set facilitates the production of almost defect-free parts with relative densities of 99.8 % and higher. The gas-atomized Ti-6Al-4V powder was provided by TLS Technik GmbH & Co. Spezialpulver KG (Bitterfeld-Wolfen, Germany). The particle size distribution of the powder, which was determined by laser diffraction, is 20 µm to 63 µm.

Table 2. L-PBF parameter set for the building the Ti-6Al-4V samples

Laser power	Scan speed	Spot diameter	Hatch distance	Layer thickness
400 W	900 mm/s	110 µm	120 µm	50 µm

The chemical composition of the powder, the sheet metal and one L-PBF sample was analyzed by energy-dispersive X-ray spectroscopy (EDS). The concentration of the metallic elements is well in accordance with the specifications given in DIN 17851 for the alloy Ti-6Al-4V (DIN 17851: Titanium alloys, Chemical Composition 1990).

The laser welding experiments were performed using a TruDisk 6001 disk laser from Trumpf GmbH + Co. KG (Ditzingen, Germany) and a PFO 33-2 focusing optics, also from Trumpf. The welding parameters were selected on basis of preliminary experiments. The selected parameter set results in sound weld seems without typical welding defects like incomplete fusion or major undercuts across.

Table 3. Parameter set for laser welding of the samples

Laser power	Welding speed	Spot diameter	Shielding gas
6000 W	7 m/min	170 µm	Argon

The samples that were designated for heat-treatment were annealed for two hours at 850 °C in argon atmosphere and slowly cooled in the furnace before and/or after welding respectively (see also Table 1). This heat-treatment was chosen based on (Vrancken et al. 2012) and already applied in previous work (Huber et al. 2019). Since the heat-treatment temperature is below the β-transus temperature of Ti-6Al-4V (Leyens and Peters 2003) no α → β phase transformation is expected. However, the α'-martensitic microstructure that forms due to the high cooling rates during L-PBF (Vrancken et al. 2012) and laser beam welding respectively (Akman et al. 2009) is supposed to be converted into an acicular α-β microstructure.

Following welding and heat-treating the tensile strength of the samples was investigated to evaluate the quality of the weld seams in dependence of the heat-treatment condition. The tensile teste were performed according to (EN ISO 6892-1 2016). The sample geometry with a rectangular cross-section, a thickness of 2 mm and a sample width of 6 mm was chosen according to (DIN 50125 2016) and was produced by milling. For the microstructural investigations the samples were cut by abrasive cutting, embedded in epoxy resin, grinded, polished with 3 µm diamond suspension and further polished with an active oxide polishing suspension (colloidal silica and hydrogenperoxide). To reveal the microstructure the polished samples were etched with Kroll's reagent (Petzow 2015). The microhardness was measured using a KB 30 S testing machine from Hegewald & Peschke Meß- und Prüftechnik GmbH (Nossen, Germany).

3. Results and Discussion

The resulting average ultimate tensile strength (UTS) of the sample groups (compare Table 1) is shown in Fig. 2. The highest UTS of 912±8 MPa was measured for welded sheet metal (SM) samples without heat-treatment. This value is well in accordance with literature (Casalino, Mortello, and Campanelli 2015). All samples fractured in the base material, hence indicating a good weld seam quality. As shown in Fig. 3 and also demonstrated in prior publications e.g. by (Kabir et al. 2012) the weld seam consists of α'-martensite which is stronger, but less ductile than the globular α-β microstructure of the base material. Consequently, the welded samples are even stronger than the non-welded sheet metal reference group with an UTS of 882±9 MPa. The α'-martensitic microstructure of the weld seam is converted into an acicular α-β

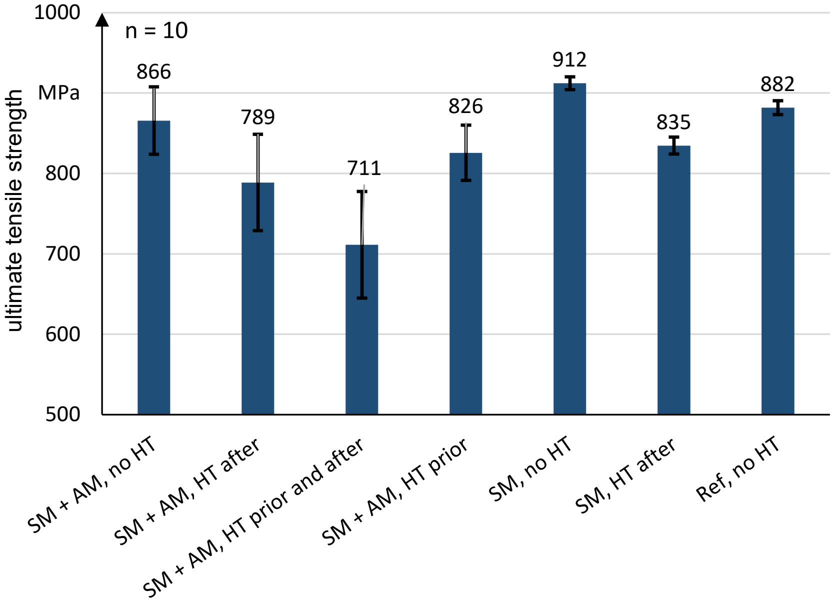

Fig. 2. Average tensile strength in dependence of the heat-treatment condition and the manufacturing process (additive manufacturing (AM) and hot rolled sheet metal (SM)); abbreviations resolved in Table 1

microstructure by the heat treatment at 850 °C. This reduces the strength but is supposed to increase toughness and ductility (Vrancken et al. 2012). As a consequence of the heat-treatment the UTS of the welded samples decreases to 835±11 MPa.

Comparing the samples welded from AM and SM with the SM-only samples similar trends can be observed. Thus, the highest UTS is measured for the non-heat-treated samples and heat-treating decreases the strength. The average UTS of the SM+AM samples is significantly lower (compare Table 4) than the average UTS of the SM-only samples with a similar heat-treatment condition. Furthermore, the standard deviation of the SM+AM samples is significantly higher (compare Table 4). Breaking of the samples occurs predominantly in the weld region, with the exception of the SM + AM, no HT samples, that break in the SM base material. This indicates, that L-PBF has a negative effect on the weld quality independently from the investigated heat-treatment states. However, no major welding defects like pores, cracks, or unmolten areas are visible in the microsections of the weld seams (see Fig. 3). Another possible explanation could be aluminum evaporation during L-PBF. However, the aluminum content of the L-PBF samples, that was determined by EDS-measurements, is in the range of 5.9±0.03 wt.% and hence only about 0.2 wt.% smaller than the aluminum content of the sheet metal. Both values are in the range defined in (DIN 17851: Titanium alloys, Chemical Composition 1990). For this reason it is assumed that the aluminum content of the L-PBF samples is not the source of the reduced tensile strength. A further possible explanation could be an increased oxygen, hydrogen or nitrogen content entrapped in the rapidly solidified L-PBF material, due to residual air or humidity in the argon atmosphere of the L-PBF machine. It can be assumed that the concentration of these elements in the hot rolled sheet metal, is lower than in the AM material. This could possibly lead to small scale defects after re-melting during welding, that are not detected by optical microscopy and would explain the lower UTS and the increased scattering of the of the values for the SM + AM welds.

Table 4. Results of U-test (test for equal mean value) and Bartlett test (test for equal variances) for SM + AM, no HT vs SM no HT and SM + AM, HT after vs SM, HT after; statistical tests performed with the software Minitab

Test	Combination	p-value
U-test	SM + AM, no HT vs SM no HT	0.000
Bartlett test	SM + AM, no HT vs SM no HT	0.000
U-test	SM + AM, HT after vs SM, HT after	0.007
Bartlett test	SM + AM, HT after vs SM, HT after	0.000

Another effect that is observed is that heat-treating of the AM samples before welding further decreases the average UTS independently whether an additional heat-treatment is performed after welding. Thus, the lowest average UTS of 711±66 MPa was measured for the sample group SM + AM, HT prior and after. A possible explanation is an additional incorporation of oxygen or nitrogen, which could lead to welding defects. A coarsening of the α-β microstructure due to the second heat-treatment was not observed.

Fig. 3 shows etched microsections of three welded samples with different heat-treatment conditions. No major welding defects like porosity or insufficient melting are observed. Only small underfill defects that are also reported in publications by (Shariff et al. 2011) or (Kabir et al. 2012) can be seen. The welds have an hourglass-like shape and a width of approximately 500 µm in the narrowest section. The heat-treatment condition of the AM-sample doesn't seem to have an impact on the morphology of the weld seams.

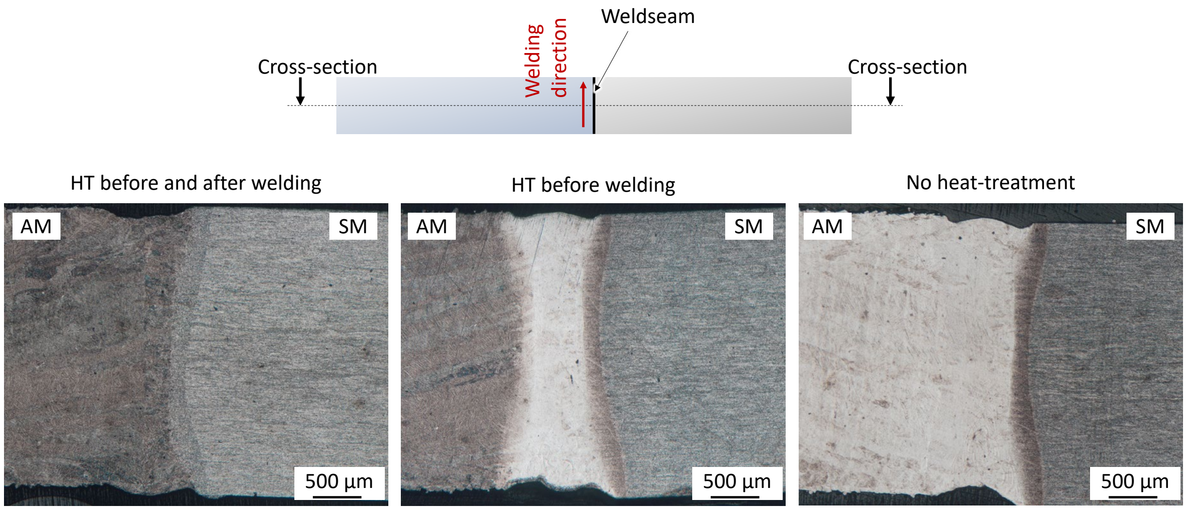

Fig. 3. Microsections perpendicular to the weld direction etched with Kroll's reagent

The microstructure and the microhardness of two AM + SM samples with and without a heat-treatment after welding was further investigated and is shown in Fig. 4. The microstructure of the sheet metal is a globular α-β microstructure (β appearing darker) with a microhardness of 322±3 HV0.01. The microstructure of the weld is α'-martensitic with a hardness of 443±16 HV0.01 and the heat affected zone (HAZ) forms a transition between the sheet metal and the α'martensitic microstructure of the weld. This was already reported e.g. by (Squillace et al. 2012). The AM material also has an α'-martensitic microstructure with a hardness similar to the weld. The HAZ between AM base material and weld can't be distinguished in the microsections (see Fig. 3 and Fig. 4). However, probably due to tempering effects and relaxation the hardness of the HAZ on the AM side is slightly reduced to 429±20 HV0.01. A transformation of α'-martensite into an α-β microstructure, as it could be expected, doesn't occur in the HAZ. It is assumed, that the necessary temperatures are not kept for a sufficient time, to facilitate this transformation. Following the heat-treatment at 850 °C the α'-martensite is completely converted into an acicular α-β microstructure as reported by (Vrancken et al. 2012). In this process the microhardness is reduced to about 370 – 380 HV0.01.

The microstructure and the microhardness of the sheet metal part stays unchanged. These microstructural changes are in good accordance to the tensile test results and explain the reduced UTS of heat-treated samples.

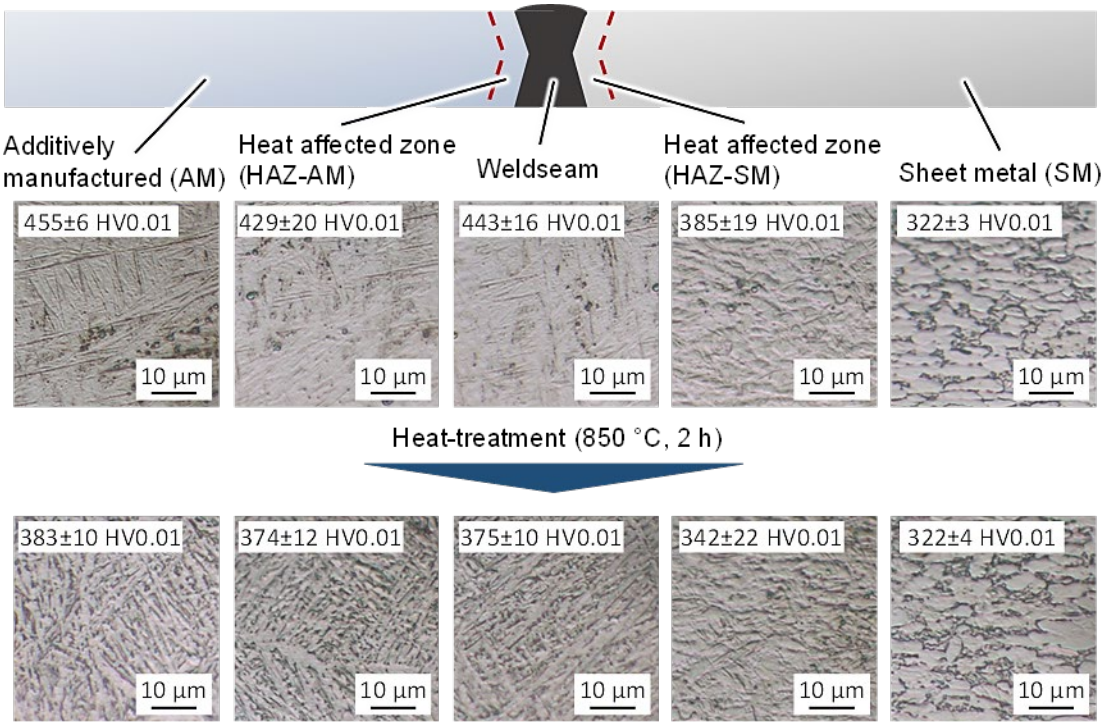

Fig. 4. Microstructure and microhardness (n = 12) of two AM + SM samples with and without a heat-treatment after welding

4. Summary

Laser beam welding of additively manufactured Ti-6Al-4V with conventionally hot rolled Ti-6Al-4V was investigated within this work. Since a heat-treatment is commonly applied after L-PBF, different heat-treatment conditions were taken into account. The heat-treatment below the β-transus temperature of Ti-6Al-4V, that was investigated, leads to a decomposition of α'-martensite in the weld seam as well as in the AM part into an acicular α-β microstructure. In the process the microhardness of the material is reduced from 440 – 450 HV0.01 to 370 – 380 HV0.01, but the toughness and the ductility is supposed to be increased.

It is shown, that sound weld seams without major welding defects like strong porosity or incomplete fusion can be produced from additively manufactured Ti-6Al-4V and sheet metal independently of the heat-treatment condition of the AM-material. However, it is observed, that AM samples show a lower ultimate tensile strength and an increased variance of the ultimate tensile strength compared to welded sheet metal (e.g. 866±41 MPa compared to 912±8MPa). This could be explained by an increased oxygen, nitrogen or hydrogen content of the L-PBF material compared to the hot rolled sheet metal, which might lead to small scale welding defects.

Furthermore, a heat-treatment before welding reduces the ultimate tensile strength of the samples no matter whether a second heat-treatment is applied after welding. One possible explanation could also be oxygen or nitrogen incorporation during the heat-treatment caused by impurities of the argon atmosphere of the furnace, which might affect the weld quality. Hence, for practical applications it is recommended to perform the heat-treatment after welding.

Acknowledgements

The authors want to thank the German Research Foundation (DFG) for funding Collaborative Research Center 814 (CRC 814), sub-project B5. Support from the Erlangen Graduate School in Advanced Optical Technologies (SAOT) in the framework of DFG's excellence initiative is gratefully acknowledged.

References

Akman, E., A. Demir, T. Canel, and T. Sınmazçelik. 2009. “Laser Welding of Ti6Al4V Titanium Alloys.” *Journal of Materials Processing Technology* 209(8): 3705–13. https://linkinghub.elsevier.com/retrieve/pii/S0924013608006572.

Baumers, Martin, Phill Dickens, Chris Tuck, and Richard Hague. 2016. “The Cost of Additive Manufacturing: Machine Productivity, Economies of Scale and Technology-Push.” *Technological Forecasting and Social Change* 102: 193–201. https://linkinghub.elsevier.com/retrieve/pii/S0040162515000530.

Brandl, Erhard, Ulrike Heckenberger, Vitus Holzinger, and Damien Buchbinder. 2012. “Additive Manufactured AlSi10Mg Samples Using Selective Laser Melting (SLM): Microstructure, High Cycle Fatigue, and Fracture Behavior.” *Materials & Design* 34: 159–69. https://linkinghub.elsevier.com/retrieve/pii/S0261306911005590.

Casalino, Giuseppe, Michelangelo Mortello, and Sabina L. Campanelli. 2015. “Ytterbium Fiber Laser Welding of Ti6Al4V Alloy.” *Journal of Manufacturing Processes* 20: 250–56. https://linkinghub.elsevier.com/retrieve/pii/S1526612515000754.

Concept Laser GmbH. 2019. “Concept Laser X LINE 2000R.” https://www.concept-laser.de/fileadmin/Blaue_Broschueren/1708_X_LINE_2000R_DE_update_2__lowres_einzel.pdf (May 14, 2019).

“DIN 17851: Titanium Alloys, Chemical Composition.” 1990.

DIN 50125. 2016. “Prüfung Metallischer Werkstoffe - Zugproben.”

EN ISO 6892-1. 2016. “Metallische Werkstoffe - Zugversuch- Prüfverfahren Bei Raumtemperatur.”

EOS GmbH. 2019. “EOS M 100 Product Data Sheet.” https://cdn0.scrvt.com/eos/8f7775003262211b/a649dae5ac8c/EOS_System_Data_Sheet_EOS_M_100_de_WEB.pdf (May 14, 2019).

Herzog, Dirk, Vanessa Seyda, Eric Wycisk, and Claus Emmelmann. 2016. “Additive Manufacturing of Metals.” *Acta Materialia* 117: 371–92. http://dx.doi.org/10.1016/j.actamat.2016.07.019.

Huber, Florian et al. 2018. “CUSTOMIZED EXPOSURE STRATEGIES FOR MANUFACTURING HYBRID PARTS BY COMBINING LASER BEAM MELTING AND SHEET METAL FORMING.” In *International Congress on Applications of Lasers & Electro-Optics (ICALEO)*, Oralndo, USA.

Jardini, André Luiz et al. 2014. “Cranial Reconstruction: 3D Biomodel and Custom-Built Implant Created Using Additive Manufacturing.” *Journal of Cranio-Maxillofacial Surgery* 42(8): 1877–84. https://linkinghub.elsevier.com/retrieve/pii/S1010518214002303.

Kabir, Abu Syed H. et al. 2012. “Effect of Postweld Heat Treatment on Microstructure, Hardness, and Tensile Properties of Laser-Welded Ti-6Al-4V.” *Metallurgical and Materials Transactions A* 43(11): 4171–84. http://link.springer.com/10.1007/s11661-012-1230-5.

Lavery, N.P. et al. 2017. “Effects of Hot Isostatic Pressing on the Elastic Modulus and Tensile Properties of 316L Parts Made by Powder Bed Laser Fusion.” *Materials Science and Engineering: A* 693: 186–213. https://linkinghub.elsevier.com/retrieve/pii/S092150931730415X.

Leyens, Christoph, and Manfred Peters. 2003. Titanium and Titanium Alloys *Titanium an Titanium Alloys*.

Petzow, Günter. 2015. *Metallographisches, Keramographisches, Plastographisches Ätzen*. 7th ed. Stuttgart: Borntaeger.

Rosswag GmbH. 2017. “ForgeBrid Der Schmiede-SLM-Hybrid.” https://www.rosswag-engineering.de/data-4/1/forgebrid.pdf (May 14, 2019).

Sadowski, Magda, Leila Ladani, William Brindley, and John Romano. 2016. “Optimizing Quality of Additively Manufactured Inconel 718 Using Powder Bed Laser Melting Process.” *Additive Manufacturing* 11: 60–70. https://linkinghub.elsevier.com/retrieve/pii/S2214860416300483.

Shariff, T et al. 2011. “Laser Welding of Ti–5Al–5V–5Mo–3Cr.” *Canadian Metallurgical Quarterly* 50(3): 263–72. http://www.tandfonline.com/doi/full/10.1179/1879139511Y.0000000009.

SLM Solutions GmbH. 2019. “SLM 500 Product Description.” https://slm-solutions.us/product/slm-500/ (May 14, 2019).

Squillace, A., U. Prisco, S. Ciliberto, and A. Astarita. 2012. “Effect of Welding Parameters on Morphology and Mechanical Properties of Ti–6Al–4V Laser Beam Welded Butt Joints.” *Journal of Materials Processing Technology* 212(2): 427–36. https://linkinghub.elsevier.com/retrieve/pii/S0924013611002871.

Thijs, Lore et al. 2010. “A Study of the Microstructural Evolution during Selective Laser Melting of Ti–6Al–4V.” *Acta Materialia* 58(9): 3303–12. https://linkinghub.elsevier.com/retrieve/pii/S135964541000090X.

Uhlmann, Eckart et al. 2015. “Additive Manufacturing of Titanium Alloy for Aircraft Components.” *Procedia CIRP* 35: 55–60. http://dx.doi.org/10.1016/j.procir.2015.08.061.

Vilaro, T., C. Colin, and J. D. Bartout. 2011. “As-Fabricated and Heat-Treated Microstructures of the Ti-6Al-4V Alloy Processed by Selective Laser Melting.” *Metallurgical and Materials Transactions A* 42(10): 3190–99. http://link.springer.com/10.1007/s11661-011-0731-y.

Vrancken, Bey, Lore Thijs, Jean Pierre Kruth, and Jan Van Humbeeck. 2012. “Heat Treatment of Ti6Al4V Produced by Selective Laser Melting: Microstructure and Mechanical Properties.” *Journal of Alloys and Compounds* 541: 177–85. http://dx.doi.org/10.1016/j.jallcom.2012.07.022.

Wohlers, Terry, Tim Caffrey, and Ian Campbell. 2016. *Wohlers Report 2016 Published*. http://wohlersassociates.com/2016report.htm.